

## Lung Deposition of Jet Engine Exhaust Particulate Matter

Elizabeth A. Black<sup>\*†</sup>, Prem Lobo<sup>‡</sup> and Donald E. Hagen<sup>§</sup>

*Center of Excellence for Aerospace Particulate Emissions Reduction Research,  
320 W. 12<sup>th</sup> Street, G7 Norwood Hall, Missouri University of Science and Technology,  
Rolla MO 65409*

**Submission Date: September 22, 2009**

<b>Word Count:</b>	<b>9,426</b>
<b>Figures:</b>	<b>12</b>
<b>Tables:</b>	<b>2</b>

---

\* Corresponding author

† e-mail: eabtg@[mst.edu](mailto:mst.edu)

‡ e-mail: plobo@[mst.edu](mailto:mst.edu)

§ e-mail: hagen@[mst.edu](mailto:mst.edu)

**ABSTRACT**

Particulate matter (PM) from on-road vehicular traffic has been correlated to increases in mortality and morbidity as PM concentrations increase. Like vehicular exhaust PM, jet engine exhaust (JEE) PM falls within the size range of interest when considering health effects. Despite this, no information currently exists on the inhalation health impact of JEE PM. JEE PM has unique properties with respect to deposition, retention kinetics, and clearance pathways in the human respiratory system, and is composed of sizes that readily travel gas streamlines that penetrate the deepest regions of the lung; this is a concern as deposited JEE PM in these regions could potentially cross the blood-membrane barrier and migrate into the bloodstream. Using JEE PM data collected during plume studies performed down-wind of active runways at the Hartsfield-Jackson Atlanta and Oakland International Airports, lung deposition probabilities of JEE PM (as a function of particle size) can be determined using the International Committee of Radiological Protection (ICRP) lung deposition model. Surface area, however, is the characteristic PM parameter most strongly correlated with health impacts. Using the deposition probabilities and size resolved number distributions, a Surface Area Deposition Index (SADI) was developed. This new parameter, SADI, quantizes JEE PM lung deposition as the surface area of deposited PM per kilogram fuel burned. As constructed, SADI allows for equitable comparison among jet engine types while also providing a surface area metric for meaningful health impact correlations. Two interesting conclusions to this preliminary study are that statistically significant differences among engine types are not seen in SADI, and variations in SADI are not correlated with temporal changes or changes in meteorological conditions.

## INTRODUCTION

Studies over the last decade have suggested that particulate matter (PM) within certain size ranges increase mortality and morbidity rates as PM concentrations become elevated (*1-4*). Commercial air traffic has increased over the last decade, and to accommodate this trend, many US airports are expanding their operations leading to increased PM concentrations in the airport complex. Thus air quality has become an important consideration for airports and their surrounding communities. While on-road vehicular PM is typically the dominant source of PM in urban areas (*5-6*), airport operations (including aircraft) can also be associated with elevated levels of PM (*7-9*).

This work is a first of a kind investigation into possible health hazards of jet engine exhaust (JEE) PM by focusing on the deposition probability of JEE PM in the deepest regions of the human respiratory system. Deposition probabilities of JEE PM were determined as a function particle size for various engine types during take-off sequences using emissions databases from airport wind transported plume studies previously performed at the Hartsfield-Jackson Atlanta International Airport (ATL) and Oakland International Airport (OAK) (*10-12*). The data used in this analysis was collected at ground level within distances comparable to those experienced by working airport ground crews and surrounding communities. A novel metric, Surface Area Deposition Index (SADI), was developed to quantify lung deposition of JEE PM. This metric allows for health impact correlations and for comparison among different emissions sources.

On-road vehicular PM is typically the dominant source of PM in urban areas and its effect on the population's health continues to be investigated. Since surface area of lung deposited PM has been correlated with health effects (*13,14*), current studies on diesel engine exhaust (DEE) identify PM surface area metrics to assist in quantifying health impacts of vehicular engine exhaust PM similarly to this work. (*15,16*) Though JEE PM and DEE PM have fundamental differences such as morphology and density, similarities do occur for PM properties that impact lung deposition. A short comparison of JEE PM and DEE PM is included in this study, and illustrates the need for further investigation into the health impact of JEE PM inhalation. In light of these parallels in deposition properties, and the current concerns of vehicular engine exhaust PM lung deposition due to its potential health effects, JEE PM should also be investigated further as a potential inhalation hazard.

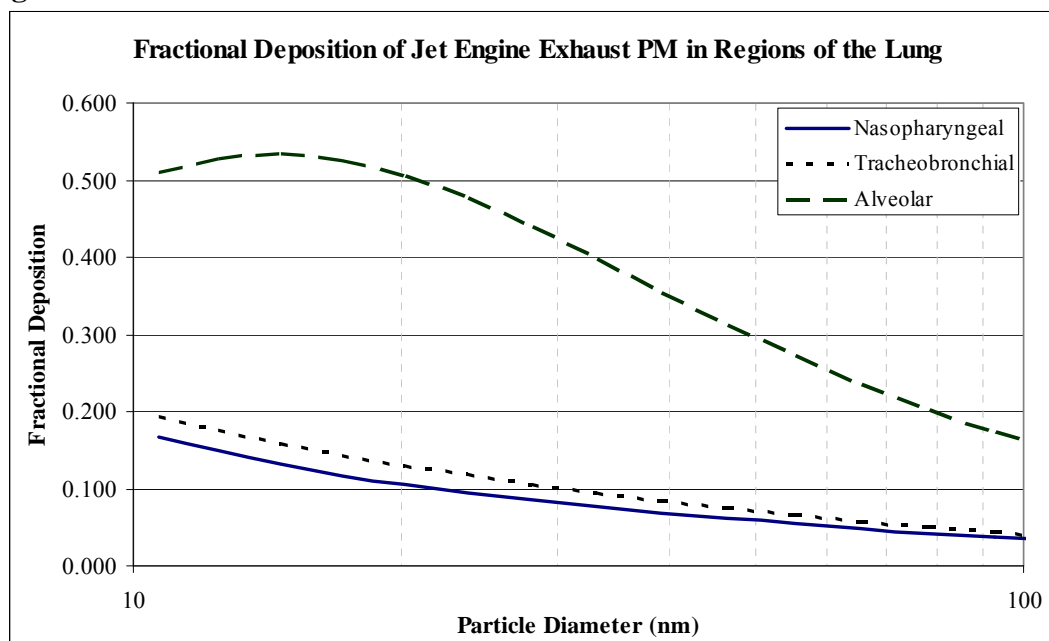
### Lung Deposition of PM

Once PM is inhaled, the human respiratory tract acts as a filter removing PM at various stages. The ability of PM to deposit in the respiratory tract can be associated with probabilities specific to each individual region of the lung (*17, 13*). Four parameters for PM are of special interest in analyzing its impact on a human that breathes it into his/her respiratory system: diameter, which controls where the particle will be deposited; surface area, which controls the effect once deposited; soluble mass fraction, which affects hygroscopic growth; and chemical composition, which determines whether there will be a negative or positive health impact upon deposition (*13, 14, 17*).

While larger particles will be removed by natural filtering and inertial effects in the nose and upper regions of the respiratory system (nasopharyngeal), smaller particles are able to follow air streamlines and reach the deepest portions of the lung (tracheobronchial and alveolar regions). For each region of the lung, the deposition probability for a particle changes as a function of particle size (*17, 18*). As seen in Figure 1, PM of 10 to 100 nm diameters have the highest fractional deposition in the alveolar region. PM deposited in the alveolar and

tracheobronchial regions have the potential to then enter the bloodstream and be transported to extra-pulmonary tissues (19, 20).

**FIGURE 1 Fractional deposition of JEE PM inhaled by a male nose breather under light working conditions.**



Health concerns arise when inhaled PM is able to deposit in the lungs and translocate throughout regions of the body. When PM is deposited in the lungs irritation and inflammation can occur as short-term symptoms. Yang et al. (2003) investigated general health of airport workers in a Taiwanese airport and found that chronic respiratory symptoms such as cough and dyspnea were heightened among male airport workers exposed to either aviation fuel or exhaust. No strong correlations, however, were found between exposure and acute irritative symptoms of the 106 male airport workers considered in that study. Long term exposure effects were not addressed and distinction was not made as to what type of exposure workers individually experienced (21). No data, however, currently exists addressing either short term or long term health effects related to aircraft specific exhaust exposure.

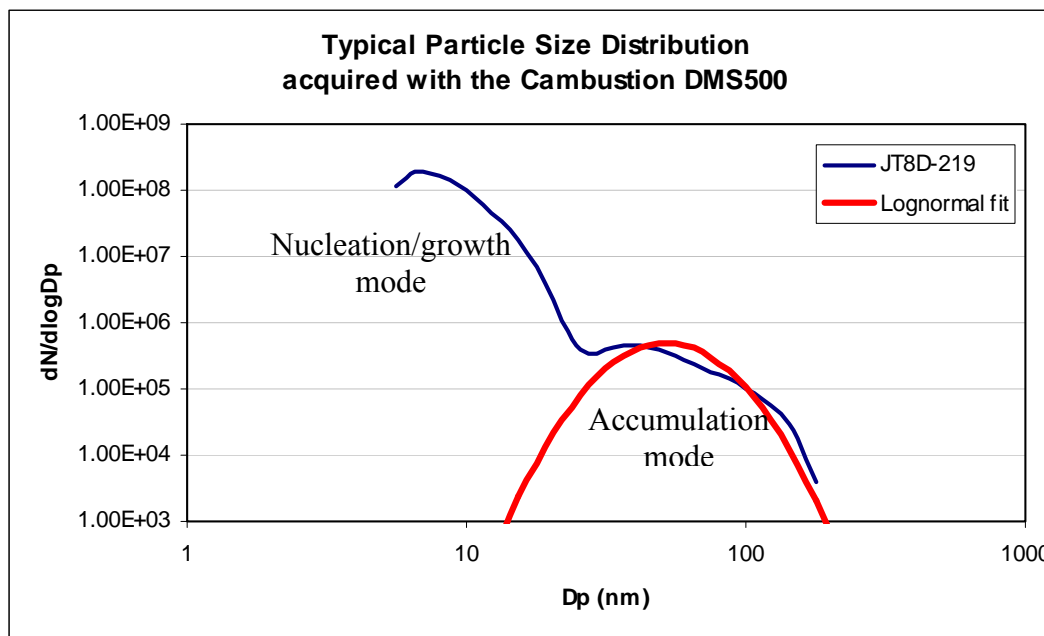
### Aircraft-Specific PM

In the aviation community, studies have focused on the measurement and modeling of emissions from jet aircraft both on the ground and at altitude. These studies have generally identified the composition and size distribution of PM produced and emitted from aircraft. Jet engines combust considerable amounts of fuel, both at cruise altitudes and near the ground during the Landing-Takeoff cycle. This releases many pollutants which include PM, nitrogen oxides ( $\text{NO}_x$ ), unburnt hydrocarbons, carbon monoxide (CO) and sulfur oxides ( $\text{SO}_x$ ). Like vehicular exhaust, these emissions have been found to evolve with increasing distance from the source (22, 23, 11). And, just as vehicular exhaust is unique to engine technology, engine operating conditions, and fuel specifications, so too are aircraft emissions (24, 25, 10). At the engine exhaust plane, the particles are essentially spherical soot cores. Other studies have also shown that as combusted particles move through the air, the PM evolves, affecting the overall size

distribution and composition of the exhaust plume. In the APEX 1 study (25), emissions were measured at various distances from the engine exit plane to determine how characteristics of PM changed as the plume expanded and mixed with ambient air. It was found that the soluble mass fraction (SMF), a measure of the fraction of PM mass that is water soluble, increased with the distance from the engine exit plane. At a distance of 30 m from the engine exit plane, it was also evident that low-vapor pressure gaseous species in the gas phase at the engine exhaust plane had been condensed to the particle phase (gas-to-particle conversion) (23). Aircraft engine exhaust also contains hydrocarbon compounds (26) of intermediate volatility which, upon oxidation in the atmosphere, produce compounds with lowered volatility (27) and contribute to secondary organic aerosol (SOA) mass. On a longer time scale the atmospheric oxidation of SO<sub>2</sub> and NO<sub>2</sub> (producing sulfuric and nitric acid, respectively) contribute to the formation of inorganic aerosol as particulate ammonium sulfate and ammonium nitrate. Thus, as PM and gaseous PM precursors travel through the ambient air and away from the emission source, the plume evolves resulting in dramatic changes in PM characteristics.

As the plume of exhaust travels through ambient air it cools, allowing for microphysical processing that changes the overall size distribution and composition of the exhaust plume. These physical reactions create PM size distributions that can generally have two distinct modes: nucleation/growth mode and accumulation mode (28). Figure 2 shows a typical size distribution of JEE with the two modes clearly distinguishable: the nucleation/growth mode at the small diameter sizes and the accumulation mode at the larger sizes of the distribution. The nucleation/growth mode is comprised primarily of soluble PM that is generally less than 20 nm in diameter and generated by gas-to-particle conversion as the wind transported plume cools and mixes with ambient air. The accumulation mode consists of the insoluble spherical carbon cores onto which sulfur and organic compounds and water vapor condense. This accumulation mode in the wind transported plume is of primary interest when considering lung deposition and potential health effects of JEE PM; the lungs have defensive mechanisms that suppress the health impact of the soluble nucleation mode.

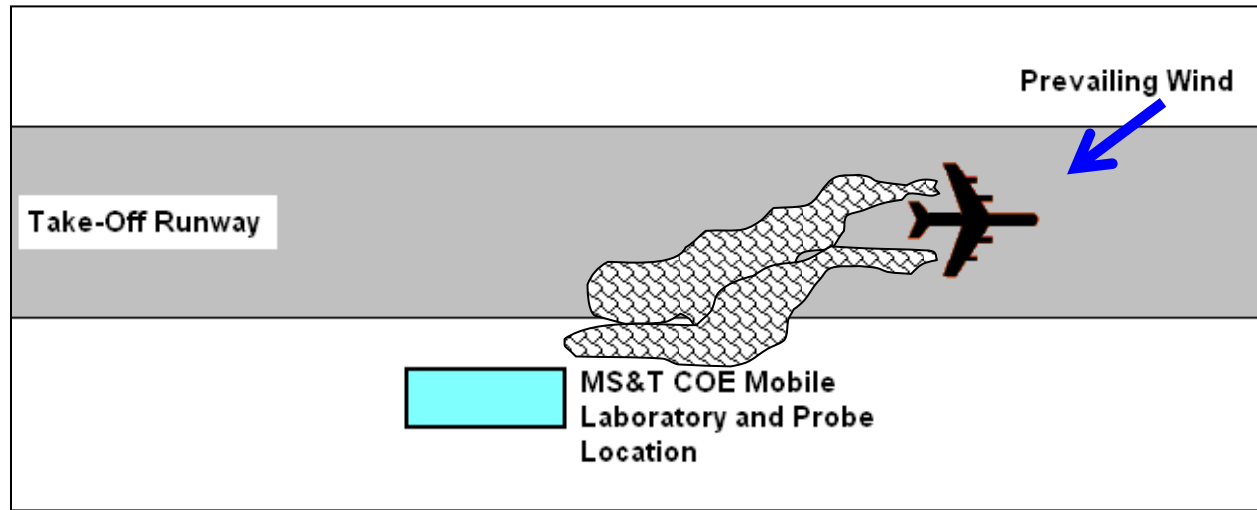
**FIGURE 2 A typical size distribution acquired using the Combustion DMS500, with a lognormal fit to the accumulation mode of the distribution.**



## METHODOLOGY

This study utilizes PM size distribution data acquired by the Missouri University of Science & Technology Center of Excellence for Aerospace Particulate Emissions Reduction Research (Missouri S&T COE), at ATL and OAK airports. As generally depicted in Figure 3, JEE PM was sampled downwind of active taxi- and runways. The sample locations were selected adjacent to airport runways at distances of 100 m or greater from take-off sites, and chosen so JEE plumes would be transported by prevailing winds to the diagnostic instrumentation. For both campaigns aircraft tail numbers were recorded for identification of airframes and engine types. Weather conditions were also monitored and recorded continuously throughout testing periods.

Sampling at ATL occurred over three days with varying meteorological conditions. Throughout the testing period 344 take-off events were identified, with the following airframe/engine combinations: B737 (CFM56), MD88 (JT8D), CL-600 (CF34), B767 (CF6-80), ATR 72(PW127), and B757 (PW2037). During the study at OAK sampling lasted for one 12 hour period. The majority of the 300 identified take-off events were associated with B737 (CFM56).

**FIGURE 3 Generalized depiction of study testing site locations.**

At each airport location, exhaust samples were extracted from the plume using a probe mounted outside the mobile laboratory housing the diagnostic instrumentation. A PM drier was included in the sampling system to remove water prior to characterization. Size distributions, total particle concentrations (TCNs), and CO<sub>2</sub> concentrations were acquired using a Cambustion DMS500 and CO<sub>2</sub> detector. The DMS500 provided high resolution real-time size distribution data and TCNs of PM, while the CO<sub>2</sub> detector provided the CO<sub>2</sub> concentrations used to establish emission factors. Further details of sampling methodology and data processing of measurements at ATL and OAK can be found elsewhere (10, 12). Of particular importance to this study and addressed here is how jet engine specific PM data was acquired and identified.

In the airport complex a number of emissions sources contribute to overall PM. In order to distinguish jet engine specific PM of aircraft take-offs from other sources, measurement of ambient PM when no aircraft activity occurred was performed throughout the testing periods. This ambient, or background, PM may be generated from vehicular traffic, industry, and even taxiing or landing events associated with other aircraft. For each aircraft related event, background PM concentrations were determined as closely to the take-off event as possible. These background PM size distributions, TCNs and CO<sub>2</sub> concentrations were then subtracted from the measured concentrations during known jet engine take-off events to yield aircraft take-off specific event data sets. Figure 2 shows a typical background subtracted size distribution from a measured JT8D engine take-off event during the ATL study.

Once background subtractions were made, the accumulation mode of the jet engine specific size distributions was extracted using a lognormal best-fit (Figure 2). These size distributions were adjusted before use in determining deposition probabilities to account for hygroscopic growth in the lung. Due to the high humidity environment of the respiratory system, PM grows as the soluble shell surrounding the carbon core absorbs water vapor. This particle growth has a significant impact on size and therefore a significant impact on deposition probabilities for the inhaled PM. The growth of the JEE PM can be accounted for using the hygroscopic growth equation from Pruppacher & Klett,(1997):

$$RH = \exp \left\{ \frac{2 \cdot M_w \cdot \sigma_{s/a} - \nu \cdot \Phi_s \cdot \epsilon_m \cdot M_w \cdot \rho_N \cdot r_N^3}{R \cdot T \cdot \rho_w \cdot a - M_s \cdot \rho_w \cdot (a^3 - r_N^3)} \right\} \quad (1)$$

where  $RH$  is the relative humidity,  $a$  is the new hydrated particle radius in cm, and  $r_N$  is the initial dry particle size radius in cm (29). All other variables are constants with values chosen under the following assumptions: the insoluble portion of PM is modeled as carbon and soluble portion as sulfate; a humidity of 99.48% is encountered immediately upon entrance into the respiratory system; and the aerosol immediately equilibrates with this humidity upon entering the body. A SMF of 0.1 for all dry particle sizes was used based on previous measurements (10). The calculated PM hydrated sizes became the input diameters to the International Committee of Radiological Protection (ICRP) lung deposition model.

The ICRP lung deposition model was initially developed to determine radiated particle doses in the medical field. This model has also been applied in health impact studies to predict PM deposition of airborne particles (30). As recently shown by Lonhdahl et al. (2009), when hygroscopicity was considered, the ICRP model accurately predicted deposition of PM samples taken at a busy intersection (30). The ICRP lung deposition model is used here to determine deposition efficiency and fractional deposition of JEE PM.

Deposition efficiency,  $\eta$ , determines the probability of PM deposition in a specific region of the lung as a function of particle size, density, and mode of inhalation (mouth or nose breathing):

$$\eta_j = 1 - \exp\{-aR^p\} \quad (2)$$

where  $\eta_j$  is the deposition efficiency of lung region  $j$ , and  $a$ ,  $R$ , and  $p$  vary by region and are defined by the ICRP model based upon the anatomical proportions of the respiratory system and work load of the inhaler (17). For this study, deposition is assumed to be carried out in adult male nose breathers under light working conditions.

The fractional deposition,  $DE$ , gives the fraction of inhaled particles that will deposit in each region of the lung once inhaled. It is determined for each region of the lung as a function of particle size using the deposition efficiency, and accounts for particles previously removed as they traveled through preceding regions of the lung:

$$DE_1 = \eta_1 \cdot I \quad (3)$$

$$DE_j = DE_{j-1} \cdot \eta_j \cdot \frac{\phi_j}{\phi_{j-1}} \left( \frac{1}{\eta_{j-1}} - 1 \right) \quad \text{where } j > 1 \quad (4)$$

where  $DE_j$  is the fractional deposition in lung region  $j$ ,  $I$  is the inhalability of a particle, and  $\phi$  is the volumetric fraction (fraction of air going through a region). The inhalability is a ratio of particles inhaled to particles in the ambient air and is a function of particle size and encountered wind speed. During the testing period, wind speeds generally did not exceed 10 m/s, allowing for the inhalability equation of Vincent et al. (1990) to be applied:

$$I = 0.5 \left[ 1 + \exp\{-0.06 \cdot d_{ae}\} \right] + 1 \times 10^{-5} \cdot U^{2.75} \cdot \exp\{0.055 \cdot d_{ae}\} \quad (5)$$

where  $d_{ae}$  is the aerodynamic particle diameter and  $U$  is the wind speed (31). In the PM size range of 10-100 nm, the inhalability remains close to unity for speeds of approximately 10 m/s or less. Figure 1 shows the fractional deposition, with inhalability of 1, for the hydrated PM sizes of consideration in this study. It is important to note that PM of size ranges 10 to 100 nm are predominantly deposited in the alveolar region.

While the fraction of particles deposited versus those sampled is of interest, this study is specifically concerned with comparisons of probabilities of PM deposited among various engine types. In order to compare different engine types relative to the amount of fuel burned, size

distributions were converted from differential concentration ( $dN/d\log D_p$ ) to differential number based emissions index size distribution ( $dEIn/d\log D_p$ ). With  $dEIn/d\log D_p$  computed for each considered size, the fractional deposition of each region is multiplied by  $dEIn/d\log D_p$  for each size bin to give the deposition index  $DI_{ij}$ . This  $DI_{ij}$  gives the concentration of particles deposited in a region  $j$  of particle size  $i$  per kilogram fuel burned.

If JEE PM deposits in the respiratory tract, the soluble portion of the particle dissociates from the carbon core. The surface area of the remaining insoluble carbon core is the primary focus for health concerns. The diameter of the insoluble carbon core is constant and is calculated using the initial original, non-hydrated, particle diameters of the accumulation mode:

$$D_u = \sqrt[3]{D_N^3 \frac{1 - SMF}{1 - SMF \left(1 - \frac{\rho_u}{\rho_s}\right)}} \quad (6)$$

where  $D_u$ ,  $\rho_u$  are the diameter and density of the insoluble portion (respectively),  $D_N$  is the dry particle diameter, and  $\rho_N$  is the density of the soluble substance (which is taken here to be sulfuric acid). Having the insoluble carbon core diameter, the surface area of the insoluble portion deposited in a given region per kilogram fuel burned can be calculated:

$$SADI_j = \pi \sum D_{u_i}^2 \Delta_i DI_{ij} \quad (7)$$

$$\Delta_i = \log(D_{u_{i+1}}) - \log(D_{u_i}) \quad (8)$$

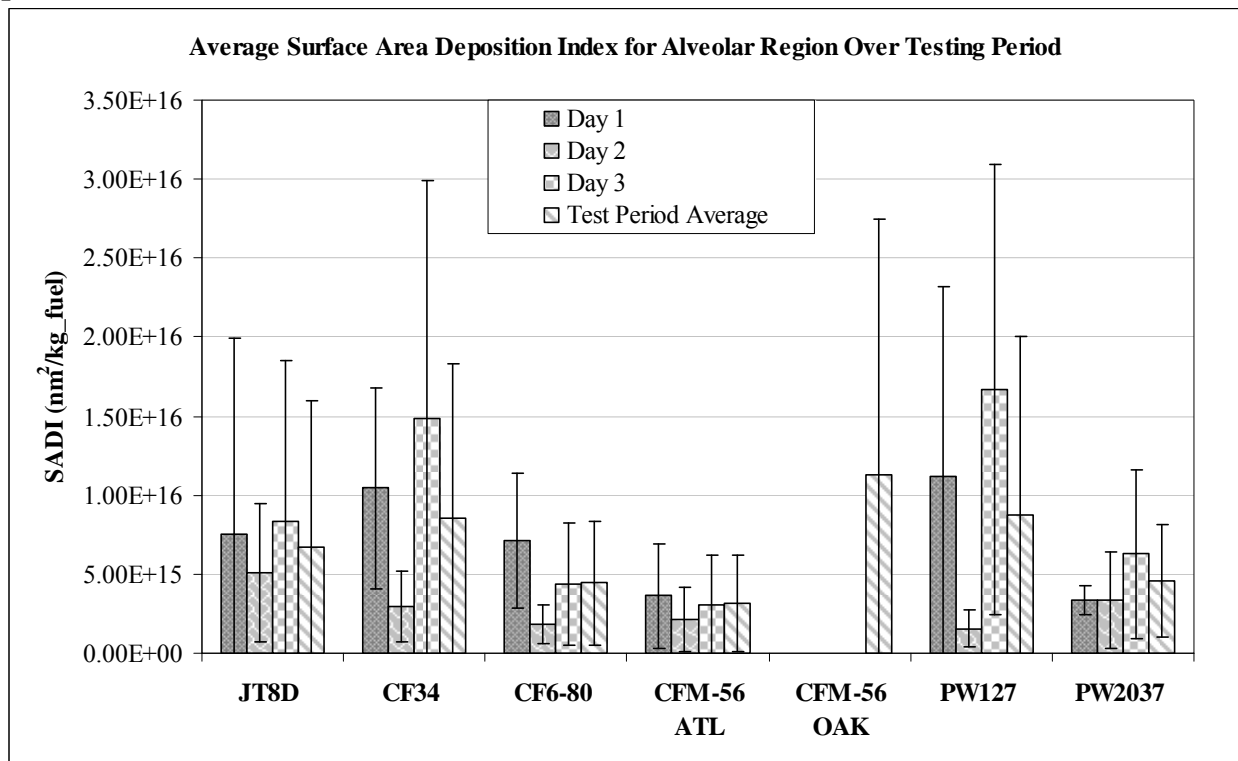
where  $SADI_j$  is the surface area deposition index and represents the surface area deposited in region  $j$  per kg fuel burned;  $DI_{ij}$  is defined above.

## RESULTS

### Surface Area Deposition Index

Studies have pointed to available particle surface area being the measurement best correlated with health effects of PM lung deposition. Therefore, a Surface Area Deposition Index (SADI) was created to compare the surface area of deposited PM among different engine types while still maintaining a useable health impact parameter. Figure 4 shows SADI averages for each engine type on a given testing day and a cumulative average for the entire test period. Certain engine types, such as the CFM56, seem to consistently be lower than the rest. Daily trends also seem apparent – the values for Day 2 are generally lower than those for Days 1 and 3 for all engine types. These trends, however, are not statistically significant as is apparent by the large error bars which represent the variability in the resulting data. Large variations are seen in SADI on a daily basis not only among different engine types, but even among engines of the same group. These large variations were not only seen in ATL data but in OAK data as well.

**Figure 4 SADI for each engine type considered, averaged per testing day and total testing period.**



Since daily averages of SADI had significant variations, the data set was examined to ascertain possible temporal trends. Figure 5 shows SADI for events over the 12 hour testing period at OAK. A consistent trend is not apparent. In Figure 7, SADI for day 1 of ATL is plotted as a function of time for the CF34, JT8D, CF6-80, PW2037, and PW127 engine types. As with the OAK data, SADI does not follow a specific trend throughout the day. Although for Figures 5 and 6, the largest peaks in SADI appear to occur at the beginning of the testing period, these peaks are not seen among all engine types and are often immediately followed by sharp drops in SADI for the next event. Hence, SADI does not appear to have any significant trends on an hourly basis during the day.

**Figure 5** Calculated SADI for each measured event of the OAK study. Each point represents the SADI calculated for the event measured at that time.

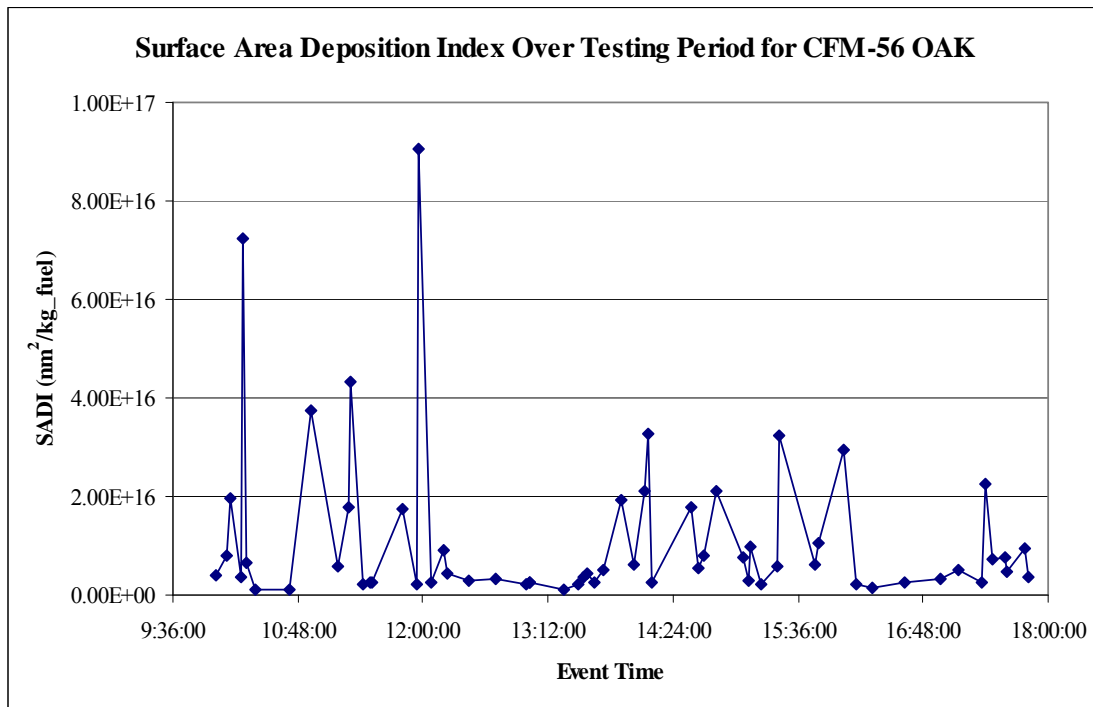
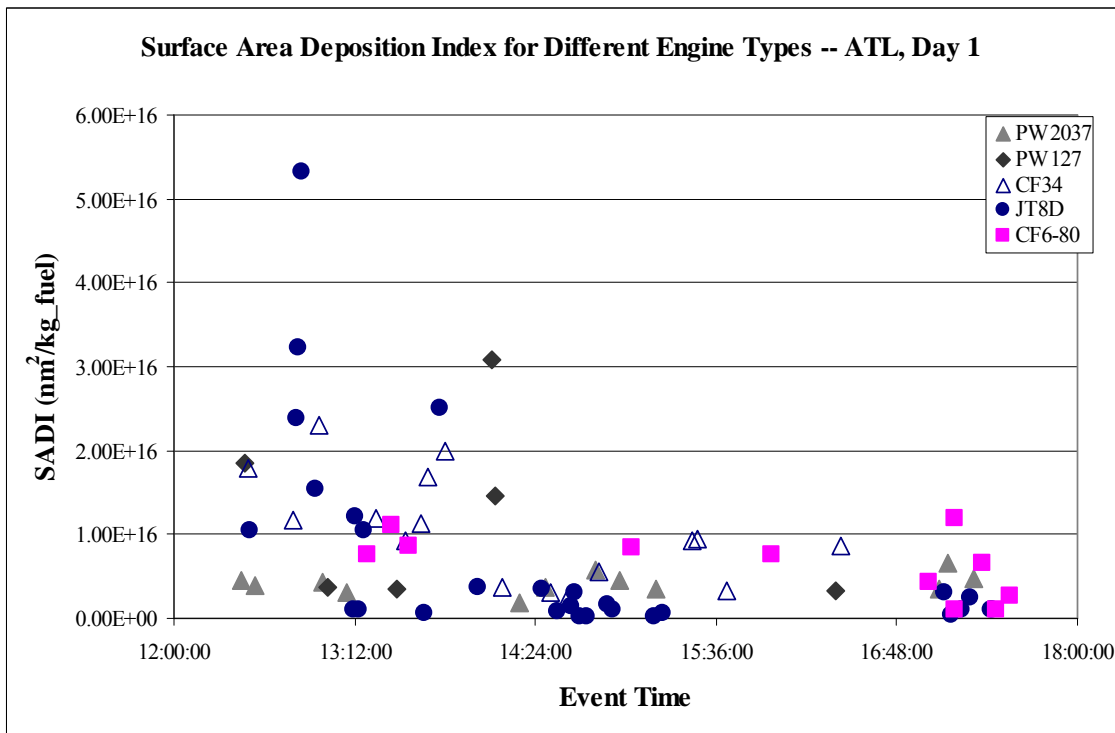


**Figure 6** Calculated SADI for ATL study events. Each point represents the SADI calculated for the event measured at that time, and is distinguished by engine type.



With daily SADI trends not observed, individual events were compared to determine factors which may be correlated with variations seen in SADI. As SADI is directly calculated from  $dE_{In}/d\log D_p$  size distributions, it is useful to view plots of  $dE_{In}/d\log D_p$  as a function of

particle diameter. Figures 7A-D compare events of the same engine type sampled on the same testing day and under similar meteorological conditions; Table 1 provides specific ambient weather conditions, geometric mean diameter (GMD) and calculated quantities of emissions index (EIn) and SADI for each event considered.

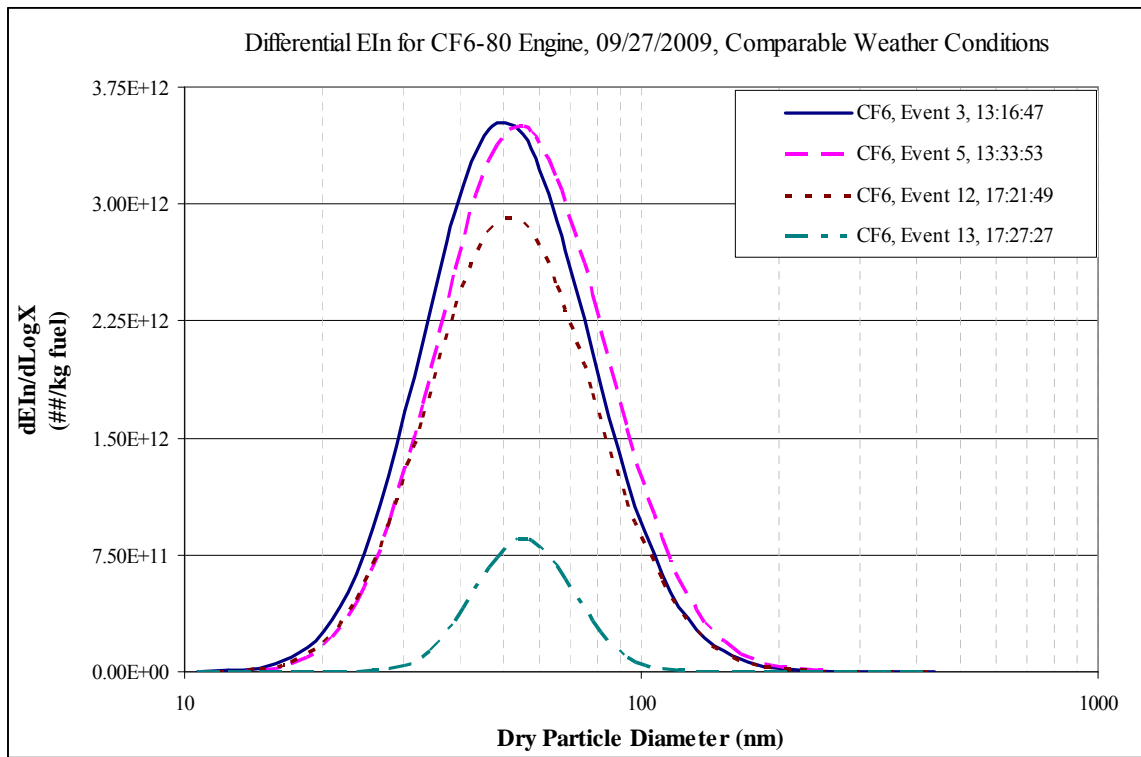
**Table 1 Parameters measured or derived during ALT testing period.**

Event	Temperature Kelvin	Pressure	% Humidity	WindSpeed (m/s)	GMD (nm)	EIn (##/kg fuel)	SADI nm <sup>2</sup> /kg fuel
<b>CF34 Engine Type</b>							
7	293	96950.00	100.00	7.67	53.02	1.53E+15	9.20E+15
12	293	96800.00	100.00	9.00	55.01	5.11E+14	3.16E+15
14	293	96750.00	100.00	7.00	55.01	9.14E+14	5.45E+15
17	293	96670.00	100.00	10.65	54.01	5.31E+14	3.24E+15
20	297	97730.00	68.60	4.48	49.01	3.93E+14	2.17E+15
22	297	97710.00	69.20	2.31	32.01	1.07E+15	3.84E+15
42	297	97890.00	51.20	4.58	58.02	2.05E+14	1.34E+15
<b>CF6-80 Engine Type</b>							
3	293	96980.00	100.00	7.77	44.02	1.51E+15	7.65E+15
5	293	96940.00	100.00	7.61	47.02	1.59E+15	8.62E+15
12	293	96610.00	100.00	7.15	45.02	1.27E+15	6.57E+15
13	293	96580.00	100.00	10.80	44.02	2.20E+14	1.08E+15
18	299	97720.00	61.00	4.53	52.01	3.99E+14	2.31E+15
23	298	97710.00	63.60	4.37	51.01	1.39E+14	7.82E+14
24	299	97700.00	55.20	5.40	51.01	4.80E+13	2.71E+14
25	298	97690.00	63.00	5.71	49.01	3.74E+14	2.06E+15

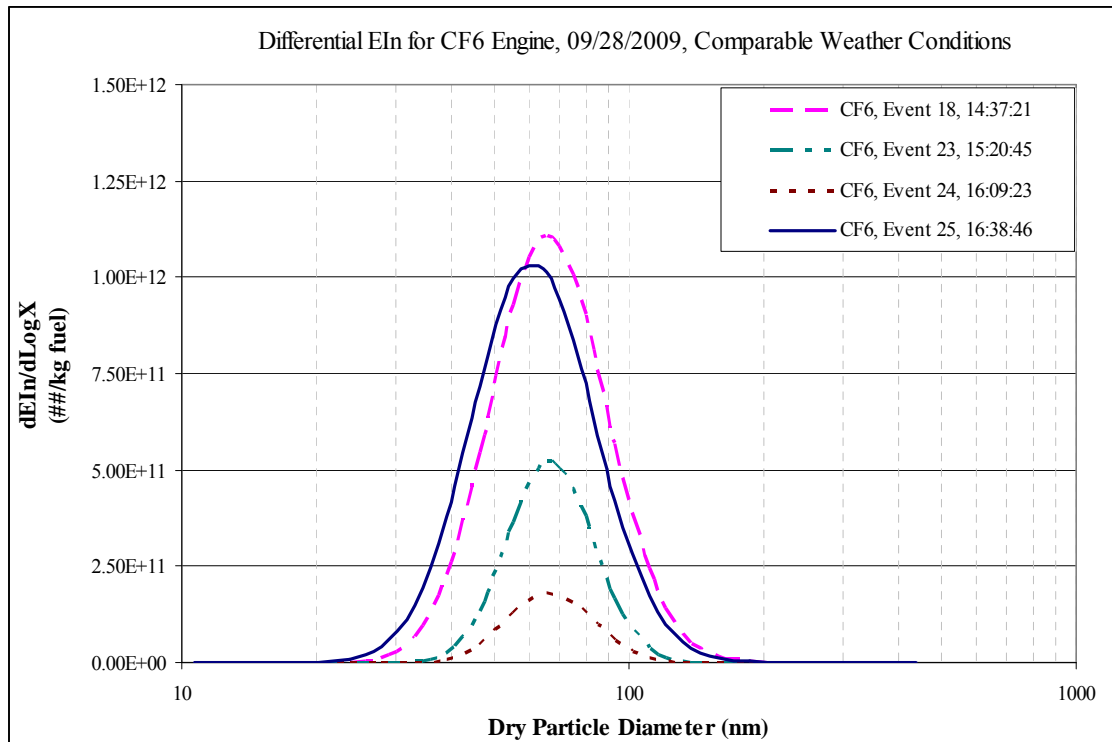
In figures 7A-D, two engine types were chosen: CF34 and CF6-80. In figure 7A, CF6-80 engine events 3, 5, 12, and 13 are compared. Events 3 and 5 were measured close to one another under similar measurement conditions of temperature, pressure, humidity, and wind speed. Under these equivalent conditions total EIn and SADI are seen to fall within the same range, with a slight deviation in GMD. Events 12 and 13 were also measured very close in time, with measurement conditions similar except for wind speed. Though GMDs for events 12 and 13 are comparable, the remaining parameters deviate drastically from one another, and SADI of event 12 almost six times greater than that of 13.

In figure 7B, CF6-80 engine events 18, 23, 24, and 25 are compared. Events were chosen for their similar meteorological measurement conditions. Though GMD shows reasonable agreement, significant differences are again seen in the EIn and SADI calculations. And, though events 18 and 25 have the greatest time span between them, these events show the greatest agreement between measured and calculated parameters.

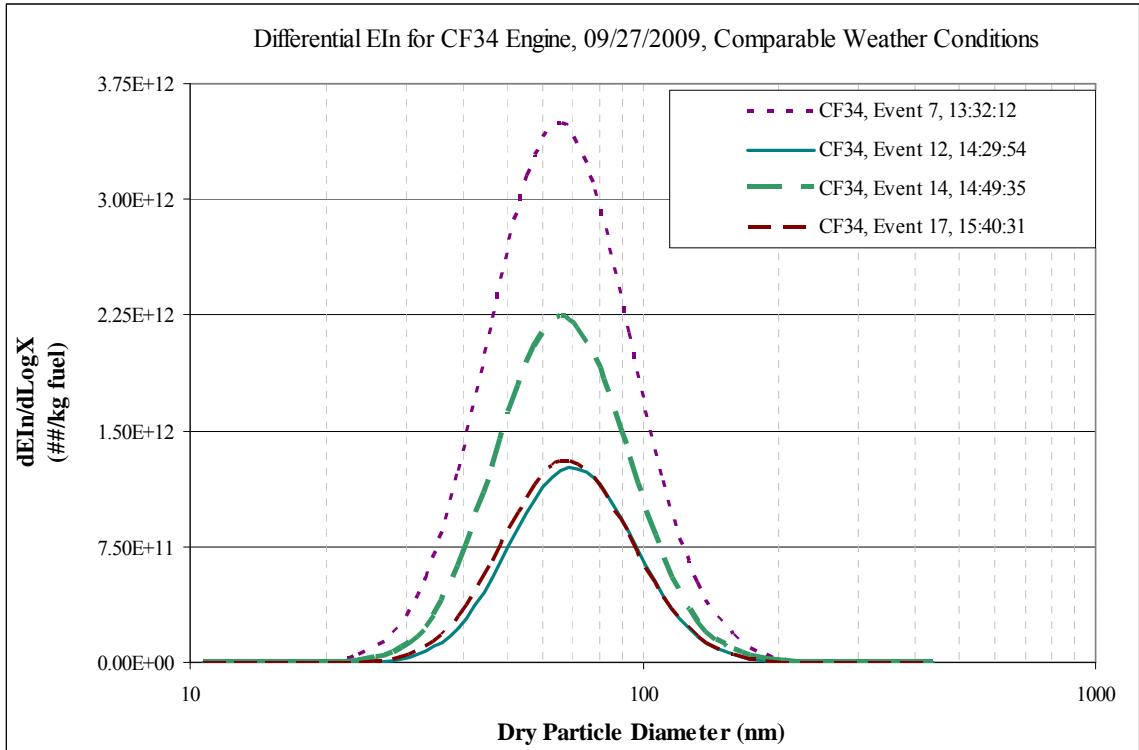
**FIGURE 7**



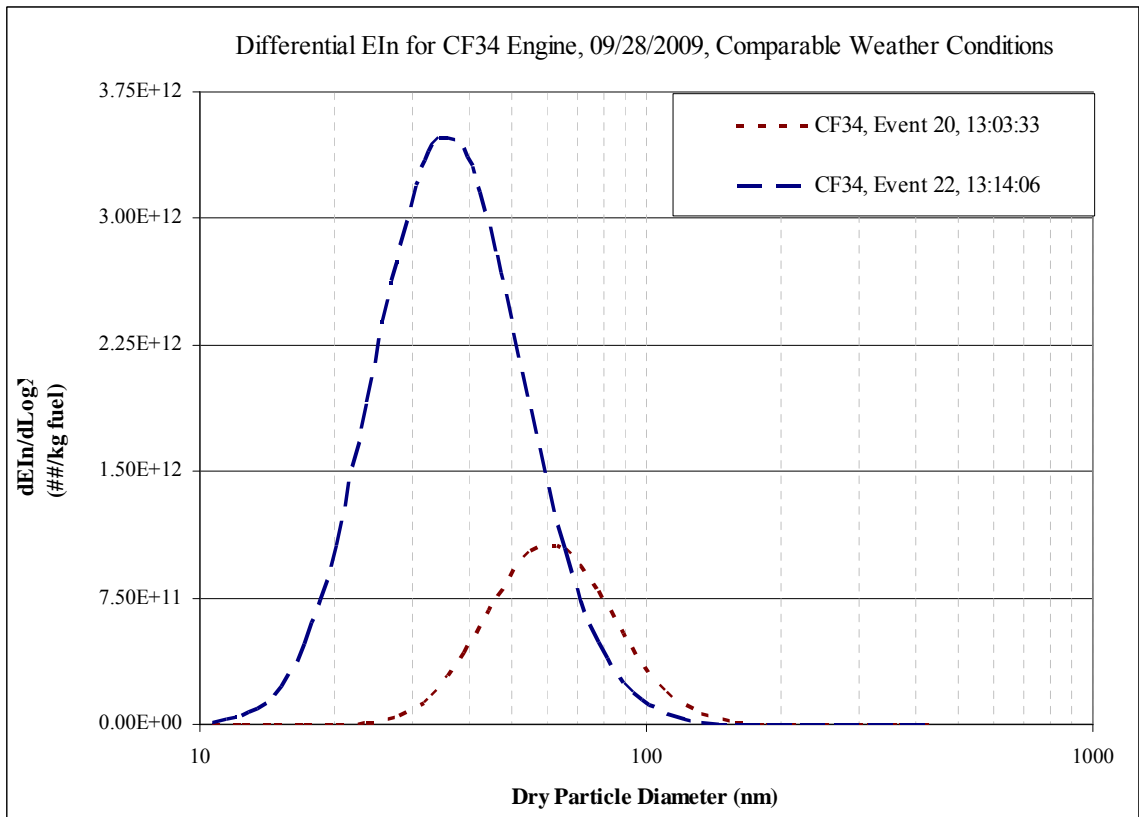
A.



B.



C.



D.

In figures 7C and 7D, CF34 engine events are compared. As with the CF6-80, despite similar sampling environment conditions, drastic differences in EIn and SADI are sometimes observed (Table 1). In figure 7D, despite sampling occurring within minutes of one another

events 20 and 22 show considerable differences in EIn and GMD. SADI differences are less pronounced, but this is due to the shift in the size distribution of event 20 toward larger particle diameters which increases surface area calculations. Event 42 is another example in which SADI is of the same order of magnitude as event 22 despite drastic differences in EIn; this is due to large particle diameters again effecting surface area calculations. While SADI may be comparable for specific events, other parameters such as EIn and GMD are not. The differences among SADI of events within the same engine type are not correlated with differences in meteorological conditions.

## **DISCUSSION**

### **Diesel Engine and Jet Engine Exhaust**

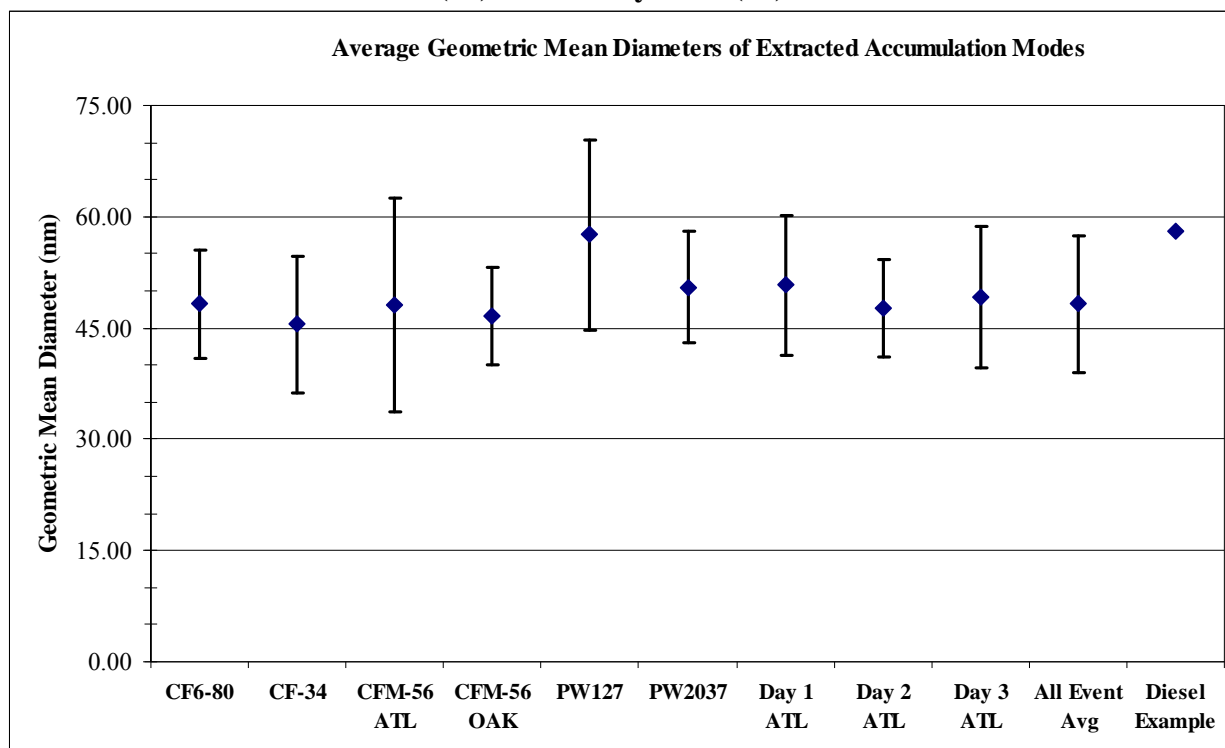
DEE PM is currently studied for its health impact upon inhalation. Health impacts of JEE PM, however, have not been investigated. Though JEE PM and DEE PM are fundamentally different, similarities occur for PM properties associated with lung deposition.

Giechaskiel et al. (15) and Alfody et al. (16) provide diesel engine accumulation mode GMD, geometric standard deviation (GSD), and TCN for three light duty diesel vehicles. Of their listed experimental conditions, case 1 was selected here to generate the DEE accumulation mode size distribution to be used in this comparison. A SMF for DEE PM is here estimated to be 0.025. The JEE PM size distribution for this comparison is taken from a CFM-56 ATL take-off event.

#### **Geometric Mean Diameters**

For each of the seven jet engine data sets, the accumulation mode was extracted from particle size distributions of sampled JEE plumes. As shown in Figure 4, each jet engine (averaged over the entire testing period) had similar average GMDs for their corresponding accumulation mode distributions. During the ATL testing period there were notable day-to-day variations in weather conditions. Despite these varying weather conditions, daily averages of GMD for all testing events still remained statistically constant (Day 1, Day 2, and Day 3 of ATL in Figure 8). The OAK data also showed good agreement with the ATL GMDs measured. In general GMDs, across engine type, showed reasonable agreement with a total sample average of 48.3 nm with standard deviation of 9.3 nm.

**FIGURE 8.** Average geometric mean diameters of accumulation modes for individual jet engine groups, all daily ATL aircraft events, total ATL and OAK events, and diesel engine as taken from Giechaskiel et al. (10) and Alfody et al. (11).



For the DEE PM size distribution, the accumulation mode GMD is 58.0 nm. Plotted in Figure 4 for comparison, the DEE accumulation mode GMD is only slightly higher than that of the JEE accumulation mode average, but the two are not statistically different since their error bars overlap.

#### Size Distributions

As listed in Table 2, the DEE PM GMD, GSD, and TCN are higher than those for the JEE CFM-56 accumulation mode before hydration is considered. Once hydration due to entrance into the high humidity of the lung is accounted for, both size distributions widen and their peaks shift to the right. The degree to which the size distributions shift varies, however, due to the different SMFs. The JEE PM size distribution moves further to the right and expands to a greater degree than the DEE size distribution. The peaks of both accumulation mode size distributions, however, remain in close proximity (within 6-7 nm of one another).

When considering deposition and retention kinetics of the lung, recall that particle size is of greatest significance. While the DEE PM accumulation mode may have a larger particle size span than that of JEE PM accumulation mode, both size distributions peak within a range associated with heightened fractional deposition in the alveolar region (1 to 100 nm). So while the DEE PM accumulation mode size distribution reaches further to the right and includes PM of larger particle sizes than that of JEE PM, these larger particles will be filtered out before reaching the alveolar region. Therefore, it is not surprising that a smaller percentage of total inhaled PM is deposited for the DEE PM, at 23.4%, than the JEE PM, at 28.5%. If looking only at particles of size 1 to 100 nm, the deposition percentage drops, with DEE PM at 21.9% and JEE PM at 26.8%, however, the deposition percentage remains higher with JEE PM.

**FIGURE 9 Accumulation mode PM size distributions of DEE and JEE.**

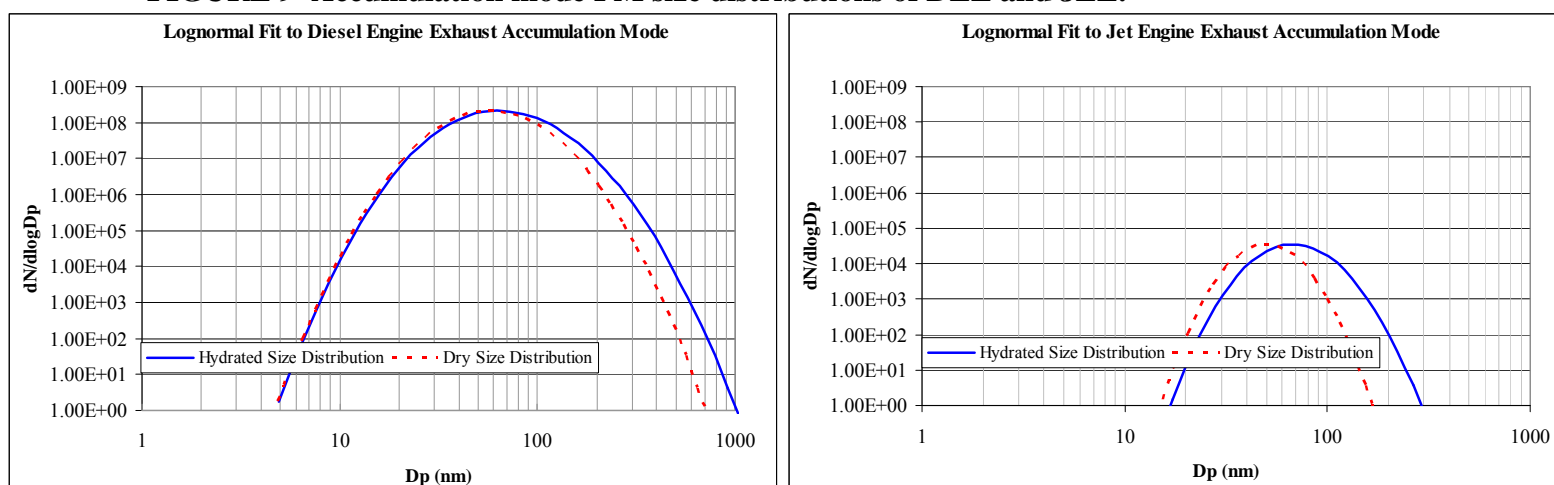


**TABLE 2 Accumulation mode PM parameters of DEE and JEE samples relating to lung deposition in the alveolar region.**

Parameter	Diesel Engine Exhaust	Jet Engine Exhaust (CFM-56)
GMD (Dry)	58.0 nm	52.0 nm
GSD (Dry)	1.71	1.45
TCN (Dry)	1.11E+08	5.50 E+04
Estimated SMF	0.025	0.10
GMD (hydrated)	64.2 nm	71.5 nm
% Deposited	23.4 %	28.5 %
% Deposited Between 1 to 100 nm	21.9 %	26.8 %

#### Total Particle Concentration

The TCN of the DEE PM accumulation mode is considerably higher than that of the JEE PM sample. It would be misleading to make any assumptions in regards to these concentration differences, however, since they arise from sampling locations. The JEE PM sample was taken downwind from aircraft along a runway. As such, the PM concentrations became greatly diluted by ambient air as they traveled to the sampling probe. The DEE PM sample provided by Giechaskiel et al. and Alfodyl et al., however, were taken directly at the vehicle's tailpipe. The overall concentration, then, is much higher since the exhaust plume did not become diluted as the JEE plume.

### Summary

On-road vehicular PM is typically the dominant source of PM in urban areas and its effect on the population's health continues to be investigated. Lung deposition within each individual region of the lung is specifically dependent upon particle size, and with both engines creating particles within the size range of greatest alveolar fractional deposition, JEE PM deposition is as likely as DEE PM deposition. For segments of the population downwind of airports the health impact studies of combustion generated PM from engines should include the role of JEE PM.

### CONCLUSIONS

A new health impact metric for JEE PM, Surface Area Deposition Index, was developed and evaluated for over 500 take-off events.

When investigating wind transported JEE PM and their deposition probabilities in the lungs, the accumulation mode is of particular interest. The accumulation mode GMD is generally consistent across different engine types and within a range corresponding to high fractional deposition in the alveolar region of the lung. Though the GMD parameter is consistent,  $dE_{in}/d\log D_p$  distributions varied considerably among engine type and within engine specific data groups. Since SADI is determined from these distributions, the variability was carried forward into SADI. These variations were not found to follow daily patterns nor correlate with changes in ambient weather conditions. This high degree of variability leads to the conclusion that there is no statistically significant difference in SADI for different engine types. Further work would be needed to understand the large variations in accumulation mode size distribution concentrations, which directly effect the calculation of SADI. This conclusion that SADI is independent of engine type is important. The negative health impact associated with JEE PM scales with fuel consumption. The focus of minimizing health impacts can be on improving engine efficiency, i.e. reducing fuel consumption.

### ACKNOWLEDGEMENTS

This work was sponsored by the Federal Aviation Administration and was conducted under the Airports Cooperative Research Program (ACRP 11-04: Graduate Research Award Program on Public-Sector Aviation Issues) administered by the Transportation Research Board of the National Academies (Project Manager: Larry Goldstein). The opinions and conclusions expressed or implied in the presentation are those of the authors. They are not necessarily those of the Transportation Research Board, the National Academies, or the program sponsor.

### REFERENCES

- (1) Norris, G., et al. An Association between Fine Particles and Asthma Emergency Department Visits for Children in Seattle. *Environmental Health Perspective*, Vol. 107, No. 6, 1999, pp. 489-493.
- (2) Samet, J.M., Dominici, F., Cureiro, F.C., Coursac, I., and Zeger, A.L. Fine Particulate Air Pollution and Mortality in 20 U.S. Cities, 1987-1994. *New England Journal of Medicine*, Vol. 343, 2000, pp. 1742-1749.

- (3) Dab, W., et al. Air Pollution and Health: Correlation or Causality? The Case of the Relationship between Exposure to Particles and Cardiopulmonary Mortality. *Journal of Air & Waste Management Association*, Vol. 51, 2001, pp. 220-235.
- (4) Zeka, A., Zanobetti, A., and Schwartz, J. Individual-Level Modifiers of the Effects of Particulate Matter on Daily Mortality. *American Journal of Epidemiology*, Vol. 163, No. 9, 2006, pp. 849-859.
- (5) Zhu, Y., Hinds, W.C., Kim, S., and Sioutas, C. Concentration and size distribution of ultrafine particles near a major highway. *Atmospheric Environment*, Vol. 36, No. 27, 2002, pp. 4323-4335.
- (6) Ying, Q., et al. Modeling air quality during the California Regional PM10/PM2.5 Air Quality Study (CPRAQS) using the UCD/CIT source-oriented air quality mode – Part III. Regional source apportionment of secondary and total airborne particulate matter. *Atmospheric Environment*, Vol. 43, 2009, pp. 419-430.
- (7) Unal, A., Hu, Y., Chang, M.E., Odman, M.T., and Russel, A.G. Airport related emissions and impacts on air quality: Application to the Atlanta International Airport. *Atmospheric Environment*, Vol. 39, 2005, pp. 5787-5798.
- (8) Westerdahl, D., Fruin, S.A., Fine, P.L., and Sioutas, C. The Los Angeles International Airport as a source of ultrafine particles and other pollutants to nearby communities. *Atmospheric Environment*. Vol. 42, No. 13, 2008, pp. 3143-3155.
- (9) Dodson, R.E., Houseman, E., Morin, B., and Levy, J. An analysis of continuous black carbon concentrations in proximity to an airport and major roadways. *Atmospheric Environment*, Vol. 43, 2009, pp. 3762-3773.
- (10) Lobo, P., et al. Delta – Atlanta Hartsfield (UNA-UNA) Study. PARTNER-COE-2008-002, February 2008.
- (11) Herndon, S., Jayne, J.T., Lobo, P., Onasch, T.B., Fleming, G., Hagen, D.E., Whitefield, P.D., Miake-Lye, R.C. Commercial aircraft engine emissions characterization of in-use aircraft at Hartsfield-Jackson Atlanta International Airport. *Environmental Science & Technology*, Vol. 42, No. 6, 2008, pp. 1877-1883.
- (12) Whitefield, P.D., P. Lobo, and D.E. Hagen. PM Emissions from Advected Aircraft Plumes at the Oakland International Airport. In *Sausen, R., A. Blum, D.S. Lee and C. Brüning (eds.): Proceedings of an International Conference on Transport, Atmosphere and Climate (TAC)*. Luxembourg, Office for Official Publications of the European Communities, ISBN 92-79-04583-0, 95-100, 2007
- (13) Oberdorster, G., Oberdorster, E., and Oberdorster, J. Nanotoxicology: An Emerging Discipline Evolving from Studies of Ultrafine Particles. *Environmental Health Perspectives*, Vol. 113, No. 7, 2005, pp. 823-839.

- (14) Stoeger, T., Reinhard, C., Takenaka, S., Schroepfel, A., Karg, E., Ritter, B., Heyder, J., and Schulz, H. Instillation of six different ultrafine carbon particles indicates a surface area threshold dose for acute lung inflammation in mice. *Environmental Health Perspectives*, Vol. 114, No. 3, 2006, pp. 328-333.
- (15) Alföldy, B., Giechaskiel, B., Hofmann, W., and Drossinos, Y. Size-distribution dependent lung deposition of diesel exhaust particles. *Aerosol Science*, Vol. 40, 2009, pp. 652-663.
- (16) Giechaskiel, B., Alföldy B., Drossinos, Y. A metric for health effects studies of diesel exhaust particles. *Aerosol Science*, Vol 40, 2009, pp. 639-651.
- (17) International Commission on Radiological Protection. *Human Respiratory Tract Model for Radiological Protection: A Report of a Task Group of the International Commission on Radiological Protection*. Annals of the ICRP, v. 24, nos. 1-3. Oxford: Pergamon, 1994.
- (18) Oberdorster, G. Pulmonary effects of inhaled ultrafine particles. *International Archive of Occupational Environmental Health*. Vol. 74, No. 1, 2001, pp. 1-8.
- (19) Nemmar, H., Vanbilloen, H., Hoylaerts, M.F., Hoet, P.H.M., Verbruggen, A., and Nemery, B. Passage of intratracheally instilled ultrafine particles from the lung into the systemic circulation in hamster. *American Journal of Respiratory and Critical Care Medicine*. Vol. 164, No. 9, 2001, pp. 1665-1668.
- (20) Nemmar, A., Hoet, P.H.M., Vanquickenborne, B., Dinsdale, D., Thomeer, M., Hoylaerts, M.F., Vanbilloen, H., Mortelmans, L., and Nemery, B. Passage of Inhaled Particle Ito the Blood Circulation in Humans. *Circulation*. Vol. 105, No. 4, 2002, pp. 411-414.
- (21) Yang, C.-Y., Chen, Y.-F., Chuang, H.-Y., Cheng, B.-H., Sung, F.-C., and Wu, T.-N. Adverse respiratory and irritant health effects in airport workers in Taiwan. *Journal of Toxicology and Environmental Health*, Vol. 66, No. 9, 2003, pp. 799-806.
- (22) Zhang, K.M., Wexler, A.S., Zhu, Y.F., Hinds, W.C., and Sioutas, C. Evolution of particle number distribution near roadways. Part II: The 'Road-to-Ambient' process. *Atmospheric Environment*, Vol. 38, No. 38, 2004, pp. 6655-6665.
- (23) Lobo, P., Hagen, D.E., Whitefield, P.D., and Alofs, D.J. Physical characterization of aerosol emissions from a commercial gas turbine engine. *Journal of Propulsion and Power*, Vol. 23, No. 5, 2007, pp. 919-929.
- (24) Kleeman, M.J., Schauer, J.J., and Cass, G.R. Size and Composition Distribution of Fine Particulate Matter Emitted from Motor Vehicles. *Environmental Science and Technology*, Vol. 34, No. 7, 2000, pp. 1132-1142.

- (25) Wey, C. C., Anderson, B. A., Wey, C., Miake-Lye, R. C., Whitefield, P., Howard, R. Overview on the Aircraft Particle Emissions eXperiment (APEX). *Journal of Propulsion and Power*, Vol. 23, 2007, pp. 898-905.
- (26) Herndon, S.C., Wood, E.C., Northway, M.J., Miake-Lye, R., Thornhill, L., Beyersdorf, A., Anderson, B.E., Dowlin, R., Dodds, W., and Knighton, W.B. Aircraft Hydrocarbon Emissions at Oakland International Airport. *Environmental Science & Technology*, Vol. 43, No. 6, 2009, pp. 1730-1736.
- (27) J.J. Kroll, J.J. and Seinfeld, J.H., *Atmospheric Environment*, Vol. **42**, 2008, pp. 3593
- (28) Kittelson, D.B. Engines and nanoparticles: A Review. *Journal of Aerosol Science*, Vol. 29, No. 5/6, 1998, pp. 575-588.
- (29) Pruppacher, Hans R., and James D. Klett. *Microphysics of Clouds and Precipitation*. Atmospheric and oceanographic sciences library, v. 18. Dordrecht: Kluwer Academic Publishers, 1997.
- (30) Lohndahl, J., et al. Experimentally Determined Human Respiratory Tract Deposition of Airborne Particles at a Busy Street. *Environmental Science & Technology*, XXXX, xxx, 2009, pp. 000-000.
- (31) Vincent, J. H., Mark, D., Miller, B. G., Armbruster, L. and Ogden, T. L. Aerosol inhalability at higher windspeeds. *Journal of Aerosol Science*, Vol. 21, 1990, pp. 577-586.